Filtering of Calcium Transients by the Endoplasmic Reticulum in Pancreatic β-Cells

Richard Bertram* and Arthur Sherman†
*Department of Mathematics and Institute of Molecular Biophysics, Florida State University, Tallahassee, Florida; and †Laboratory of Biological Modeling, National Institute of Diabetes and Digestive and Kidney Diseases, National Institutes of Health, Bethesda, Maryland

ABSTRACT Calcium handling in pancreatic β-cells is important for intracellular signaling, the control of electrical activity, and insulin secretion. The endoplasmic reticulum (ER) is a key organelle involved in the storage and release of intracellular Ca^{2+}. Using mathematical modeling, we analyze the filtering properties of the ER and clarify the dual role that it plays as both a Ca^{2+} source and a Ca^{2+} sink. We demonstrate that recent time-dependent data on the free Ca^{2+} concentration in pancreatic islets and β-cell clusters can be explained with a model that uses a passive ER that takes up Ca^{2+} when the cell is depolarized and the cytosolic Ca^{2+} concentration is elevated, and releases Ca^{2+} when the cell is repolarized and the cytosolic Ca^{2+} is at a lower concentration. We find that Ca^{2+}-induced Ca^{2+} release is not necessary to explain the data, and indeed the model is inconsistent with the data if Ca^{2+}-induced Ca^{2+} release is a dominating factor. Finally, we show that a three-compartment model that includes a subspace compartment between the ER and the plasma membrane provides the best agreement with the experimental Ca^{2+} data.

INTRODUCTION

A key element of glucose homeostasis is the secretion of insulin by pancreatic β-cells in response to changes in the blood glucose level. The signal transduction from external glucose to insulin secretion is a multistep process, involving cell depolarization and a subsequent elevation of the intracellular Ca^{2+} concentration. Specifically, glucose is transported across the cell membrane and metabolized, resulting in an increase in the intracellular ATP/ADP ratio. This increased ratio closes ATP-sensitive K^+ channels, depolarizing the cell and activating voltage-dependent Ca^{2+} channels. The resulting Ca^{2+} influx increases the intracellular Ca^{2+} concentration and evokes exocytosis of insulin granules (Ashcroft and Rorsman, 1989).

While Ca^{2+} influx is clearly important in the β-cell's response to depolarization, there is a large body of evidence that the endoplasmic reticulum (ER) also plays a role (Arredouani et al., 2002b; Bertram et al., 1995; Gilon et al., 1999; Lemmens et al., 2001; Miura et al., 1997; Tengholm et al., 2001). The contribution that the ER makes to Ca^{2+} handling in pancreatic islets was the focus, in particular, of a recent study in which the free cytosolic Ca^{2+} concentration was measured during an oscillatory potassium pulse protocol. Each K^+ pulse depolarizes the islet, and at the end of the pulse the cell repolarizes. The oscillatory pattern of K^+ pulses was chosen to resemble electrical bursting patterns typically observed in islets (Arredouani et al., 2002b). By controlling the electrical subsystem, the authors were able to focus on the Ca^{2+} dynamics. Calcium rose during each depolarization and decayed to a level above baseline during each repolarization. Experiments were repeated in the presence of the SERCA pump inhibitor thapsigargin (Tg), which blocks uptake of Ca^{2+} into the ER and ultimately leads to Ca^{2+} depletion in the organelle. In the presence of Tg, the amplitude of the Ca^{2+} response to depolarization was increased significantly, and the Ca^{2+} nadir between depolarizations was close to the baseline level. In a related study using longer depolarizations, Gilon et al. (1999) also demonstrated that Tg increases the amplitude of the Ca^{2+} response, and additionally increases the rate of rise of Ca^{2+} during the depolarization. Another study demonstrated that the Ca^{2+} dynamics in SERCA3 knockout mice are similar to those in control mice in the presence of Tg during short burst-like K^+ pulses, suggesting that SERCA3 is the SERCA isoform primarily responsible for filling the ER when the cytosolic Ca^{2+} concentration is elevated by depolarization (Arredouani et al., 2002a).

In this study we use mathematical modeling to address several questions related to the contribution of the ER to Ca^{2+} handling in β-cells. First, we ask whether a simple model with two Ca^{2+} compartments, the ER and cytosol, can account for the recent Ca^{2+} data of Arredouani et al. (2002b) and Gilon et al. (1999). Second, whereas these authors focused on the effects of SERCA blockers, we ask what effect other modulators such as carbachol, Li^+, and calmidazolium would have on the cytosolic Ca^{2+} dynamics. Carbachol promotes efflux of Ca^{2+} from the ER via the production of inositol 1,4,5-trisphosphate (IP_3), whereas Li^+ and calmidazolium inhibit Ca^{2+} exchangers and pumps in the plasma membrane, respectively (Nadal et al., 1994; Wolf et al., 1988). Third, we use the experimental data to constrain the speed at which the ER takes up and releases Ca^{2+}, and find that ER Ca^{2+} must be much slower than cytosolic Ca^{2+}, but not too slow.

Submitted August 4, 2004, and accepted for publication September 23, 2004.
Address reprint requests to Richard Bertram, Tel.: 850-644-7195; E-mail: bertram@math.fsu.edu.

0006-3495/04/12/3775/11 $2.00
doi: 10.1529/biophysj.104.050955

Some have suggested that calcium-induced calcium release (CICR) from the ER is important in β-cells (Ämmälä et al., 1991; Gromada et al., 1996; Kang and Holz, 2003; Lemmens et al., 2001), and indeed there is little doubt that it is important when agonists such as acetylcholine or GLP-1 are present (Ämmälä et al., 1991; Gilon et al., 1995; Gromada et al., 1996; Kang and Holz, 2003; Lemmens et al., 2001). However, in the absence of these agonists the significance of CICR is unclear. A recent study (Beauvois et al., 2004) failed to find any CICR during brief depolarizations (<40 s) such as those that occur during a burst of action potentials. Also, mRNA for ryanodine receptors, the primary mechanism for CICR in the absence of cholinergic agonists, was only weakly expressed in β-cells. However, an atypical form of CICR was observed, which was not dependent on either IP_3R or RyR, in response to supraphysiological KCl pulses, much longer and stronger than the ones in Arredouani et al. (2002b) that we simulate. This atypical CICR appeared only infrequently in response to glucose-induced calcium oscillations and was not required for those oscillations.

In the analysis presented here, we find that a passive two-compartment model (cytosol and ER only) is able to account for all of the recent time-dependent Ca^{2+} data. Thus, the Ca^{2+} filtering properties of an ER with a Ca^{2+}-dependent SERCA and slow passive leak that depends on the gradient between the ER and cytosolic Ca^{2+} levels accounts for the reported effects of Tg on the cytosolic Ca^{2+} during trains of depolarizations. Although CICR is not necessary, a modest CICR contribution is compatible with the data. However, if CICR is dominant, such that the ER drains during depolarization and refills during repolarization, then the model does not reproduce the Ca^{2+} data. Thus, if CICR is present in β-cells during normal glucose stimulation, then it must be present at modest levels.

The simple two-compartment model predicts that during long sustained depolarizations the cytosolic Ca^{2+} concentration will approach the same value with or without SERCA pump blockers. This is true whether or not CICR is present. Thus, whereas the SERCA pumping rate has a profound effect on the dynamics of the cytosolic Ca^{2+}, it has no impact on the equilibrium level of cytosolic Ca^{2+}. A slightly more complex model, called the *subspace model*, on the other hand, predicts that the measured equilibrium Ca^{2+} concentration will be lower when the ER is depleted of Ca^{2+}. The subspace model postulates that Ca^{2+} from the ER is released primarily into a compartment that lies between the ER and the plasma membrane and was motivated by the observation that a slow K^+ current ($I_{K(slow)}$) activated by burst-like trains of depolarizations (Goforth et al., 2002; Göpel et al., 1999; Kanno et al., 2002) is inhibited by SERCA pump blockade (Goforth et al., 2002). Our results suggest that the three-compartment subspace model is superior to a two-compartment model with or without CICR in reproducing the recent data on Ca^{2+} handling in β-cells.

METHODS

Basic two-compartment model

Whereas the experimental data that we simulate comes from intact islets, we use a single-cell model in our simulations. Although some phenomena, such as asynchronous Ca^{2+} releases, cannot be modeled with this approach, it suffices to explain most aspects of islet behavior because the cells are electrically coupled and their electrical activity and Ca^{2+} dynamics are synchronized. The basic two-compartment model is illustrated in Fig. 1 *A*. Calcium enters the cell through L-type Ca^{2+} channels in the plasma membrane, with flux (J_{in}) proportional to the Ca^{2+} current. Calcium is removed by Ca^{2+} pumps in the membrane, with flux (J_{pmca}) assumed to be proportional to the cytosolic free Ca^{2+} concentration (C). Thus,

$$J_{in} = -\alpha I_{Ca},\ J_{pmca} = k_{pmca}C, \tag{1}$$

where α converts current to concentration, and k_{pmca} is the plasma membrane pump rate. The Ca^{2+} current is voltage (V)-dependent, and is given by

$$I_{Ca} = g_{Ca}m(V - V_{Ca}), \tag{2}$$

where g_{Ca} is the whole cell conductance, V_{Ca} is the Ca^{2+} reversal potential, and m is the channel activation variable. Since channel activation is known to be rapid, we assume for simplicity that it is instantaneous, so $m = m_\infty\ (V) = 1/(1+e^{(v_m - V)/s_m})$.

Calcium from the cytosol is transported into the ER by SERCA pumps in the ER membrane. Two SERCA genes are expressed in β-cells, SERCA2b and SERCA3. The SERCA2b ATPase has high Ca^{2+} affinity and is primarily responsible for setting the basal level of Ca^{2+} in the ER (Varadi and Rutter, 2002). The SERCA3 ATPase has lower Ca^{2+} affinity and is primarily responsible for transporting Ca^{2+} from the cytosol to the ER during Ca^{2+} elevations, such as those produced by bursts of action potentials (Arredouani et al., 2002a). We include terms for both SERCA2b and SERCA3 in our model. Flux through SERCA2b pumps is described by a small constant term (this pump is treated as saturated even at basal cytosolic Ca^{2+} levels), whereas flux through SERCA3 pumps is assumed to be proportional to C. Flux out of the ER ($J_{release}$) is assumed to be proportional to the gradient between the concentrations of free cytosolic Ca^{2+} and free ER Ca^{2+} (C_{er}). Thus,

$$J_{serca} = k_{serca2b} + k_{serca3}C,\ J_{release} = p_{er}(C_{er} - C), \tag{3}$$

where $k_{serca2b}$ and k_{serca3} are the SERCA2b and SERCA3 rate constants, and p_{er} is the rate of Ca^{2+} release from the ER. Release from the ER could be through inositol 1,4,5-trisphophate (IP_3) or ryanodine channels in the ER membrane, or some other route of passive leak. Thapsigargin (Tg) is modeled by setting both $k_{serca2b}$ and k_{serca3} to 0, whereas SERCA3 knockout is modeled by setting only k_{serca3} to 0. The simple linear expressions used for

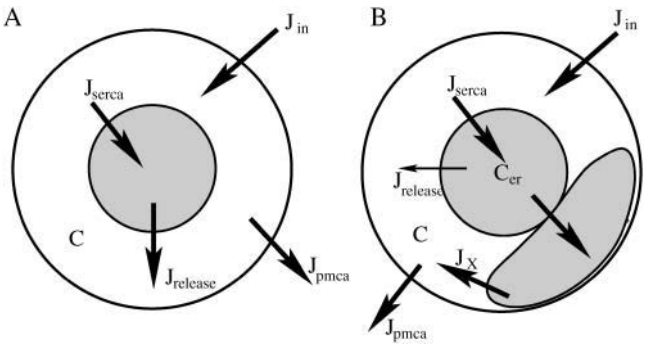

FIGURE 1 Illustration of the Ca^{2+} fluxes incorporated in (*A*) the two-compartment model and (*B*) the three-compartment subspace model. The thin arrow in *B* represents a small flux from the ER to the bulk cytosol.

ER fluxes demonstrate that no nonlinearities in the fluxes are needed to account for the data of Arredouani et al. (2002b). Similar linear ER fluxes were used by Gall and Susa (1999), but without the constant for SERCA2b.

The time-dependent concentrations of C and C_{er} are described using conservation equations. Thus,

$$\frac{dC}{dt} = f_{cyt}(J_{in} - J_{pmca} - J_{serca} + J_{release}) \quad (4)$$

$$\frac{dC_{er}}{dt} = \frac{f_{er}}{v_{er}}(v_{cyt}J_{serca} - v_{cyt}J_{release}), \quad (5)$$

where f_{cyt}, f_{er} are the fractions of free Ca^{2+} in the cytosolic and ER compartments, respectively, and ν_{cyt} and ν_{er} are the volumes of the cytosolic and ER compartments. All parameter values are listed in Table 1. The basic two-compartment model is used in Figs. 2–8.

Two-compartment model with CICR

In simulations performed with the basic two-compartment model the ER Ca^{2+} release rate, p_{er}, is constant. In simulations involving calcium-induced Ca^{2+} release (CICR), p_{er} is an increasing function of C,

$$p_{er} = p_{min} + \frac{p_{max} - p_{min}}{1 + (K_{cicr}/C)^2}, \quad (6)$$

which is constructed so that Ca^{2+} efflux from the ER is increased when cytosolic Ca^{2+} is elevated. The model with CICR is used in Figs. 9 and 10.

Three-compartment subspace model

The subspace model (Goforth et al., 2002) was motivated by experimental evidence for a Ca^{2+}-activated K^+ current ($I_{K(slow)}$) that develops during burst-like voltage-clamp depolarizations (Goforth et al., 2002; Göpel et al., 1999; Kanno et al., 2002). In this model, Ca^{2+} released from the ER primarily enters a subspace compartment adjacent to the plasma membrane, and from here can enter the bulk cytosol (Fig. 1 *B*). The Ca^{2+} concentration in the subspace (C_{ss}) is elevated compared with the bulk cytosolic Ca^{2+} (C) due to this preferential influx from the ER. Here, we assume that there is also some release from the ER directly into the bulk cytosol. In Goforth et al. (2002) it was proposed that the Ca^{2+}-activated K^+ channels that comprise a large component of $I_{K(slow)}$ respond to this elevated C_{ss} rather than the lower bulk cytosolic Ca^{2+}. We are interested here only in the Ca^{2+} handling, so ion channels other than the L-type channels are omitted from the model.

The Ca^{2+} flux terms in the subspace model are largely the same as in the two-compartment model, with the exception of the two release terms $J_{release,ss}$ and $J_{release,cyt}$, and the new flux term between the subspace and the bulk cytosol (J_X). Thus,

$$J_{release,ss} = p_{er,ss}(C_{er} - C_{ss}) \quad (7)$$

$$J_{release,cyt} = p_{er,cyt}(C_{er} - C) \quad (8)$$

$$J_X = p_X(C_{ss} - C), \quad (9)$$

TABLE 1 Parameter values used in two-compartment model

g_{Ca}	1200 pS	V_{Ca}	30 mV	α	4.5×10^{-6} μM fA^{-1} ms^{-1}
v_m	−15 mV	s_m	8 mV	f_{cyt}	0.01
f_{er}	0.01	v_{cyt}	10 μm^3	v_{er}	0.4 μm^3
p_{er}	10^{-4} ms^{-1}	p_{min}	10^{-5} ms^{-1}	p_{max}	3×10^{-4} ms^{-1}
K_{cicr}	0.5 μM	k_{pmca}	0.08 ms^{-1}	k_{serca3}	0.08 ms^{-1}
$k_{serca2b}$	0.02 μM ms^{-1}				

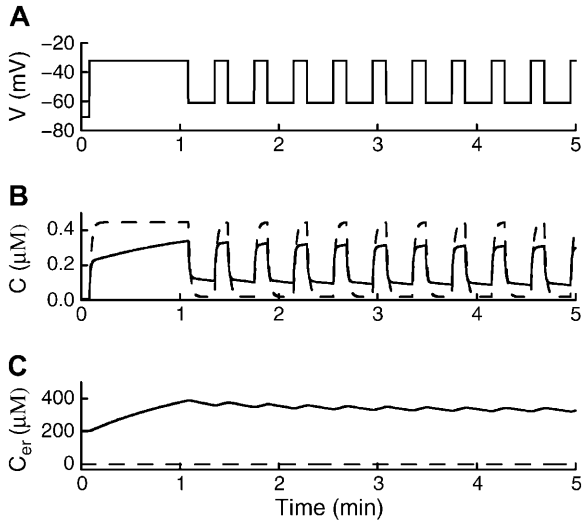

FIGURE 2 (*A*) Simulated voltage protocol mimicking the biphasic response to an increase in glucose concentration. (*B*) Cytosolic Ca^{2+} response with SERCA pumps enabled (*solid line*) and disabled (*dashed line*). During each imposed oscillation, the nadir is defined as the lowest value of C during the repolarized phase. The amplitude is the difference between the peak and the nadir. (*C*) The ER Ca^{2+} concentration. No driving force is established between the ER and the cytosol when SERCA pumps are disabled (*dashed line*).

where $p_{er,ss}$, $p_{er,cyt}$, and p_X are constants. The differential equations describing the Ca^{2+} concentrations in the three compartments are

$$\frac{dC}{dt} = f_{cyt}(J_{in} - J_{pmca} - J_{serca} + J_{release,cyt} + J_X) \quad (10)$$

$$\frac{dC_{er}}{dt} = \frac{f_{er}}{v_{er}}(v_{cyt}J_{serca} - v_{cyt}J_{release,cyt} - v_{er}J_{release,ss}) \quad (11)$$

$$\frac{dC_{ss}}{dt} = \frac{f_{ss}}{v_{ss}}(v_{er}J_{release,ss} - v_{cyt}J_X), \quad (12)$$

where f_{ss} is the fraction of free Ca^{2+} in the subspace and ν_{ss} is the volume. The observable for this model is the average of the Ca^{2+} concentrations in the bulk cytosol and the subspace compartment weighted by the compartment volumes,

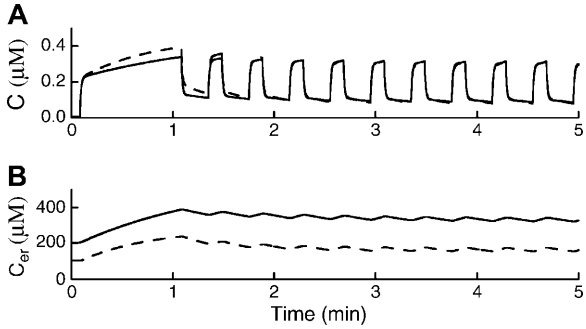

FIGURE 3 (*A*) Doubling the rate of Ca^{2+} release from the ER, p_{er}, has a transient effect on the cytosolic Ca^{2+} response (*dashed line*) to the voltage protocol, but no long-term effect. (*B*) C_{er} adapts to the doubling in p_{er} (*dashed line*) by declining to a value one-half that of the control.

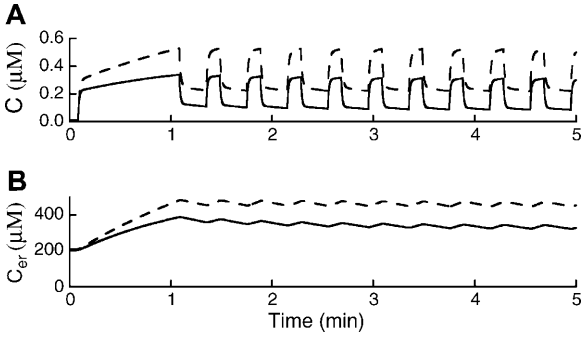

FIGURE 4 (*A*) Reducing the rate of pumping across the plasma membrane by half (*dashed line*) slightly increases the amplitude of the Ca^{2+} response to depolarization and greatly increases the Ca^{2+} nadir. (*B*) The increase in the Ca^{2+} nadir is due to an increase in C_{er}.

$$C_{avg} = \frac{v_{ss}C_{ss} + v_{cyt}C}{v_{ss} + v_{cyt}}. \tag{13}$$

All parameters for the subspace model are given in Table 2. This model is used in Fig. 11 only.

RESULTS

Ca^{2+} flux terms have differential effects on the Ca^{2+} profile

In the in vitro studies of pancreatic islets, when the bath glucose concentration is raised from a substimulatory to a suprastimulatory level the β-cell electrical response is typically biphasic. The cells first spike continuously for 1–2 min (phase 1), and then produce bursts of action potentials (phase 2) with periods ranging from 10 s to ~1 min (Meissner and Atwater, 1976). This behavior was mimicked using K^+ pulses in the experimental study by Arredouani et al. (2002b), and the average intracellular free Ca^{2+} concentration was measured. Each K^+ pulse depolarizes the islet, and the islet repolarizes between pulses. Hence, the K^+ pulse protocol is similar to a voltage-clamp protocol, with the advantage that it is applicable to intact islets. We simulated this voltage-clamp-like protocol with our mathematical models. As illustrated in Fig. 2 *A*, voltage is initially maintained at a resting potential of −70 mV. It is then

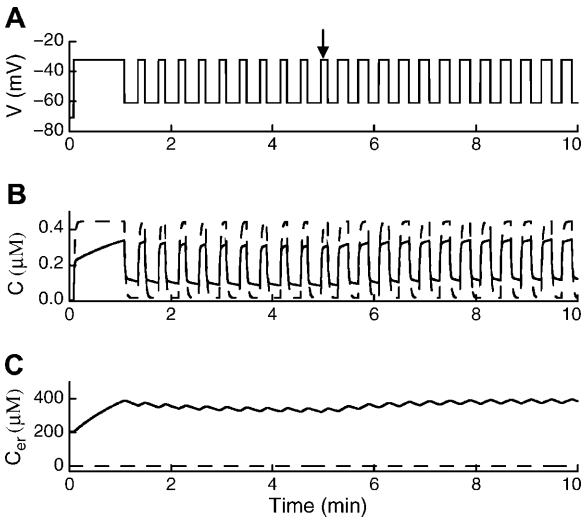

FIGURE 5 (*A*) An increase in the glucose concentration is mimicked (at *arrow*) by increasing the depolarized phase duration from 8 s to 12 s, while keeping the oscillation period fixed at 24 s. (*B*) In the control simulation (*solid line*), increasing the duration of depolarization results in an increase in the Ca^{2+} nadir, but not in the amplitude, whereas there is no effect when SERCA pumps are disabled (*dashed line*). (*C*) In the control simulation, an increase in the ER Ca^{2+} concentration is responsible for the increased cytosolic Ca^{2+} nadir.

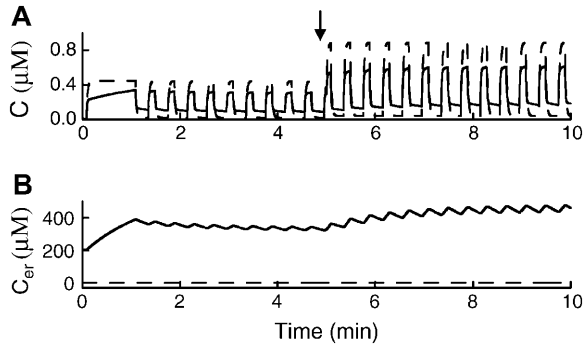

FIGURE 6 (*A*) When the Ca^{2+} channel conductance, g_{Ca}, is doubled (at *arrow*), both the Ca^{2+} amplitude and nadir are increased. This is true with SERCA pumps enabled (*solid line*) or disabled (*dashed line*), although the nadir increase in the latter case is quite small. (*B*) As in Fig. 5, the nadir increase is due primarily to an increase in the ER Ca^{2+} concentration, although increased Ca^{2+} entry also plays a role.

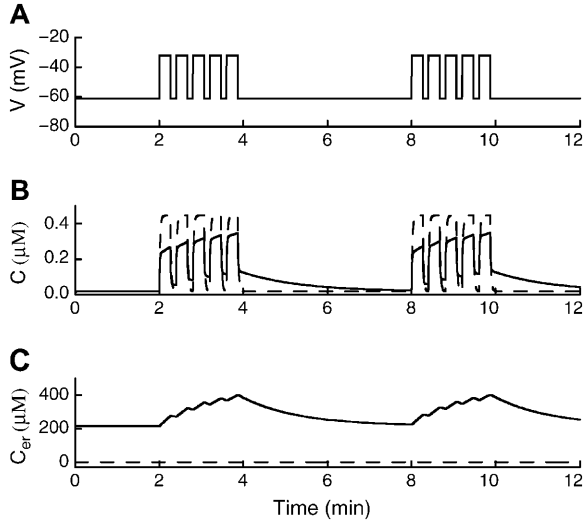

FIGURE 7 (*A*) Voltage protocol for compound bursting. (*B*) In the control system the Ca^{2+} nadir rises during a compound burst and slowly falls between (*solid line*). This does not occur when the SERCA pumps are disabled (*dashed line*). (*C*) The rise and fall of the nadir reflects the dynamics of ER Ca^{2+}.

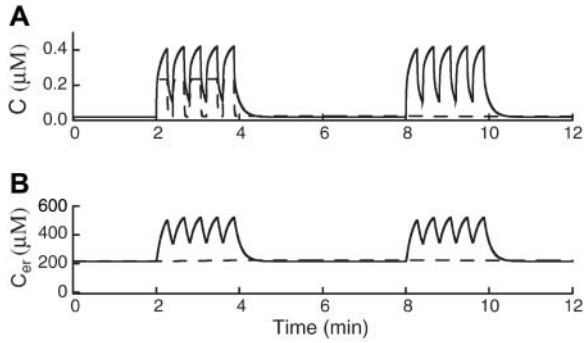

FIGURE 8 Demonstration that the slow rise and fall of the cytosolic Ca^{2+} nadir depends critically on the speed at which the ER takes up and releases Ca^{2+}. (*A*) The speed of the ER is increased by setting $f_{er} = 0.1$ (*solid line*), or decreased by setting $f_{er} = 0.0002$ (*dashed line*). (*B*) There are no slow C_{er} dynamics when $f_{er} = 0.1$, and there is only a small increase in C_{er} during a compound burst when $f_{er} = 0.0002$.

elevated to −30 mV for 1 min, mimicking the first phase of electrical activity. After this, a voltage oscillation is imposed by periodically clamping *V* between −60 mV and −30 mV, mimicking the silent and active phases of bursting, respectively. The duration of the repolarized phase is 16 s, and that of the depolarized phase is 8 s.

The model cytosolic Ca^{2+} response to this protocol is shown in Fig. 2 *B* (*solid curve*), using the basic two-compartment model without CICR. (This model is used to generate Figs. 2–8.) Note that the Ca^{2+} nadir during the silent phases is elevated above the resting level. Also note the slow rise in Ca^{2+} during the initial depolarization, which reflects the time constant of ER filling. The model ER Ca^{2+} concentration is shown in Fig. 2 *C*. During the initial

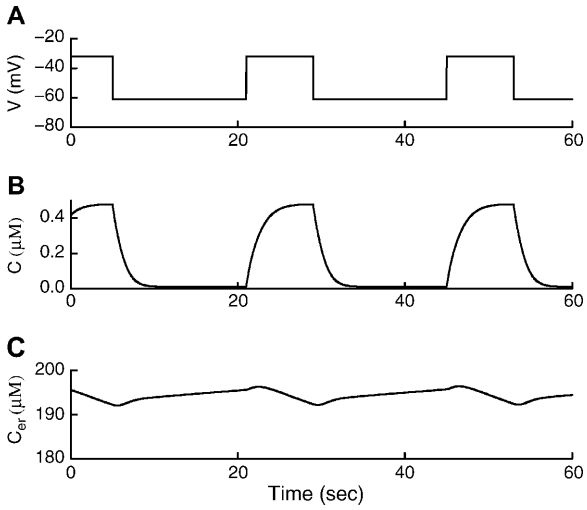

FIGURE 9 Ca^{2+} response to a sequence of depolarizations when CICR dominates release from the ER. (*A*) Sequence of brief depolarizations. (*B*) Cytosolic Ca^{2+} rises during depolarization and falls during repolarization. (*C*) The ER releases Ca^{2+} during the depolarization due to CICR, and refills during the repolarization.

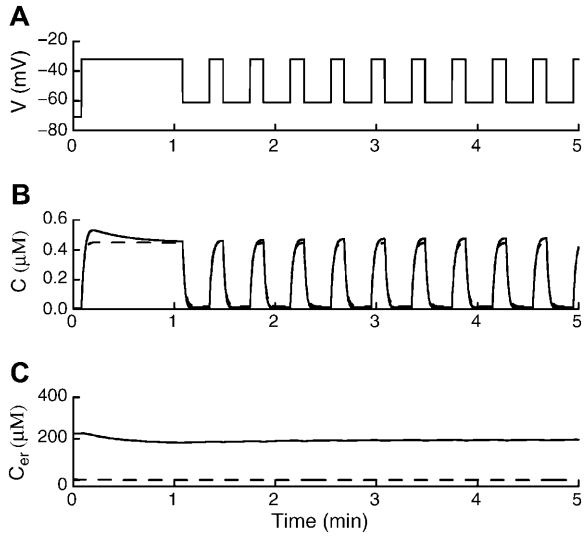

FIGURE 10 (*A*) Biphasic voltage protocol applied to the model in which CICR dominates. (*B*) Even with active SERCA pumps the Ca^{2+} nadir is not elevated and the amplitude is large (*solid line*), so that blocking SERCA pumps has only a small effect (*dashed line*). (*C*) The cytosolic Ca^{2+} nadir is not elevated despite the fact that the ER is filled.

depolarization the ER fills, and during subsequent oscillatory activity C_{er} remains elevated. This maintained elevation of C_{er} provides the driving force for a net flux of Ca^{2+} from the ER into the cytosol during the repolarized phases of the oscillatory activity, elevating the cytosolic Ca^{2+} nadir.

Application of the SERCA pump blocker thapsigargin (Tg) is simulated by setting both $k_{serca2b}$ and k_{serca3} to 0 and allowing the system to equilibrate at the resting potential, so that the cytosolic and ER Ca^{2+} concentrations converge. When the voltage protocol is applied, the amplitude of the cytosolic Ca^{2+} response is much greater and the nadir is no longer elevated (Fig. 2 *B*, *dashed curve*). This twofold effect of blocking SERCA pumps reflects two important dynamical roles of the ER. First, the ER acts as a Ca^{2+} sink, slowing the rise of cytosolic Ca^{2+}. When SERCA pumps are blocked, the filtering of cytosolic Ca^{2+} is reduced and *C* rises to a higher level. Second, the ER acts as a Ca^{2+} source when the cell is repolarized and there is little or no entry of Ca^{2+} into the cell. This latter role requires that a gradient be established between the ER and the cytosol, and this does not happen when SERCA pumps are blocked.

TABLE 2 Parameter values used in the three-compartment subspace model

g_{Ca}	1450 pS	V_{Ca}	30 mV	A	4.5×10^{-6} μM fA^{-1} ms^{-1}
k_{pmca}	0.12 ms^{-1}	k_{serca3}	0.3 ms^{-1}	$k_{serca2b}$	0.02 μM ms^{-1}
f_{cyt}	0.01	f_{er}	0.01	f_{ss}	0.01
p_X	0.045 ms^{-1}	$p_{er,cyt}$	5×10^{-5} ms^{-1}	$p_{er,ss}$	1.5×10^{-6} ms^{-1}
ν_{cyt}	3.2 μm^3	ν_{er}	0.4 μm^3	ν_{ss}	0.8 μm^3
s_m	8 mV	v_m	−13 mV		

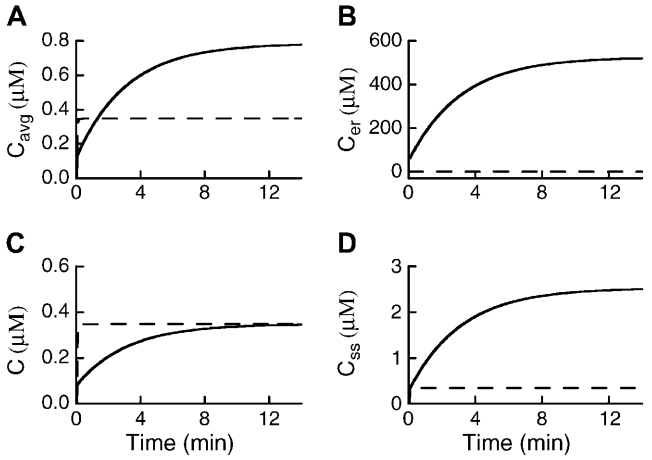

FIGURE 11 Ca^{2+} concentrations during a sustained depolarization from −70 mV to −30 mV with the three-compartment subspace model. (*A*) The weighted average of the bulk cytosolic Ca^{2+} and the subspace Ca^{2+} concentrations is lower when SERCA pumps are inhibited (*dashed line*) than in the control system (*solid line*). The ER Ca^{2+} concentration (*B*) and the subspace Ca^{2+} concentration (*D*) are lower when SERCA pumps are inhibited. (*C*) The bulk cytosolic concentration satisfies Eq. 16, so its steady state is independent of the C_{er} or ER parameters.

The simulation results in Fig. 2 reproduce the experimental data (Fig. 2, *B* and *C*, of Arredouani et al., 2002b, and Fig. 2 *A* of Gilon et al., 1999) very well, indicating that the simple two-compartment model with passive Ca^{2+} release from the ER is sufficient to describe the effects on cytosolic Ca^{2+} of disabling the SERCA pumps. Similar effects on cytosolic Ca^{2+} were observed in SERCA3 knockout mice (Arredouani et al., 2002b) and can be simulated with the model by setting $k_{serca3} = 0$ (not shown). However, the model indicates that the ER does not empty in that case, demonstrating that it is the rise and fall of ER Ca^{2+}, not the level of ER Ca^{2+}, that governs the filtering effect of the ER.

Another way to reduce C_{er} is to increase the release rate from the ER. We investigated whether increasing the Ca^{2+} release rate would increase the cytosolic Ca^{2+} amplitude and decrease the nadir during the voltage protocol, as did blocking the SERCA pumps. This was tested by doubling p_{er}. Fig. 3 shows the control response (*solid line*) and the response with p_{er} doubled (*dashed line*). Increasing the Ca^{2+} release rate had no effect on the cytosolic Ca^{2+} amplitude, and although the nadir is initially elevated, this effect is only transient. The lack of effect on the Ca^{2+} amplitude is explained by noting that the Ca^{2+} influx into the ER during a depolarization is mainly determined by $k_{serca2b}$ and k_{serca3}, not p_{er}. The lack of a long-term effect on the Ca^{2+} nadir can be understood by noting that $J_{release} = p_{er}(C_{er} - C) \approx p_{er}C_{er}$. When p_{er} is doubled C_{er} adapts by falling to half its control value (Fig. 3 *B*), and $J_{release}$ is ultimately the same as in the control simulation. Thus, the nadir is ultimately the same as in the control simulation. This model prediction can be readily tested experimentally by applying carbachol or some other muscarinic agonist to stimulate IP_3 production and increase Ca^{2+} release from the ER through IP_3 channels.

We next examined the effects of partially disabling the plasma membrane Ca^{2+} pumps by reducing k_{pmca} by half. Although this maneuver did cause a small increase in the cytosolic Ca^{2+} amplitude in response to the pulse protocol, it raised the Ca^{2+} nadir by a much larger amount (Fig. 4 *A*). The former effect is due to the reduced pumping, whereas the latter effect is due to the increased Ca^{2+} release from the ER during the repolarized phase of the oscillation. Indeed, the main consequence of reducing pumping out of the cell is to increase C so that more Ca^{2+} gets pumped into the ER, setting up a larger gradient between the ER and cytosol compartments (Fig. 4 *B*). As a result, when the cell is repolarized the ER is a greater source of Ca^{2+}, increasing the cytosolic Ca^{2+} nadir above its control value. This model prediction can be tested experimentally by replacing Na^+ with Li^+ to inhibit Na^+/Ca^{2+} exchange (Nadal et al., 1994) or applying calmidazolium to inhibit calmodulin and thus the plasma membrane Ca^{2+} pumps (Wolf et al., 1988).

In summary, reducing the uptake of Ca^{2+} into the ER by disabling the SERCA pumps yields an increased cytosolic Ca^{2+} amplitude and reduced nadir in response to the voltage protocol, consistent with the effects of the SERCA pump blocker Tg or SERCA3 knockout during a similar K^+ pulse protocol (Arredouani et al., 2002a,b). Increasing Ca^{2+} efflux from the ER has only a transient effect on the Ca^{2+} nadir; ultimately the Ca^{2+} nadir returns to its control level. Decreasing the Ca^{2+} efflux from the cell by partially inhibiting plasma membrane Ca^{2+} pumps yields a slightly increased Ca^{2+} amplitude and a significantly increased Ca^{2+} nadir in response to the voltage protocol. Thus, alterations in the level of Ca^{2+} release from the ER or in the plasma membrane pump rate have effects on the cytosolic Ca^{2+} that are quite different from the effect of disabling SERCA pumps. All of these effects can be understood in terms of the dual role of the ER as a Ca^{2+} sink and a Ca^{2+} source.

The effects of increased Ca^{2+} entry depend on how entry is increased

When the bath glucose concentration is increased from one suprastimulatory level to a higher level pancreatic islets typically respond by increasing the plateau fraction of bursting, i.e., the ratio of active phase duration to the total burst period. This effect on the membrane potential was mimicked by Arredouani et al. (2002b) by increasing the K^+ pulse duration while keeping the oscillation period fixed. (The effects of increasing the glucose concentration on pumps were found to be negligible compared to the effect on the plateau fraction.) We simulate this by increasing the depolarized duration from 8 to 12 s while decreasing the repolarized duration from 16 to 12 s, so that the oscillation period remains fixed at 24 s (Fig. 5 *A*). In the control simulation (SERCA intact), the increase in plateau fraction

causes an increase in the Ca^{2+} nadir, with little change in the Ca^{2+} amplitude (Fig. 5 *B*). This is consistent with data shown in Fig. 3 *A* of Arredouani et al. (2002b). The cause of the nadir increase is a greater influx of Ca^{2+} into the cell, and consequently a higher concentration of Ca^{2+} in the ER (Fig. 5 *C*). Thus, release of Ca^{2+} from the ER is greater during the repolarized phase, yielding an increased Ca^{2+} nadir. The Ca^{2+} amplitude is not increased by the longer depolarization because *C* equilibrates rapidly to the depolarized voltage; it has already nearly equilibrated by the end of an 8-s depolarization, so increasing the duration of depolarization will not significantly increase the cytosolic Ca^{2+} amplitude.

When the simulation is repeated with SERCA pumps disabled (Fig. 5 *B*, *dashed line*) there is again little change in the Ca^{2+} amplitude when the plateau fraction is increased. However, unlike the control simulation, the Ca^{2+} nadir is almost unchanged by the increased plateau fraction. This simulation is consistent with Fig. 3 *B* of Arredouani et al. (2002b).

Increasing the plateau fraction is one way to increase the total Ca^{2+} entry into the β-cell. Another way to do this is to increase influx through the Ca^{2+} channels. Arredouani et al. (2002b) achieved this by raising the external Ca^{2+} concentration. The approach we take in the simulations shown in Fig. 6 is to increase the Ca^{2+} channel conductance. In the control simulation, doubling g_{Ca} increases both the Ca^{2+} nadir and amplitude (Fig. 6 *A*). As when the plateau fraction was increased, the nadir is increased primarily because C_{er} is elevated (Fig. 6 *B*). An increase in the Ca^{2+} influx during the repolarized phase adds an additional (small) component to the nadir, which is evident as a small nadir increase when the SERCA pumps are disabled (*dashed line*). The increased Ca^{2+} amplitude is evident whether the SERCA pumps are enabled or disabled, and is due to an increase in the Ca^{2+} entry per unit time. Thus, in contrast to the effects of doubling the plateau fraction (Fig. 5), where the total Ca^{2+} entry is increased by increasing the duration of cell depolarization (and not the Ca^{2+} entry per unit time), increasing the conductance increases the influx (J_{in}) relative to efflux (J_{pmca}) during the depolarized phase, resulting in an increased Ca^{2+} amplitude. Results from this simulation, both in control and with SERCA pumps inhibited, are consistent with data in Fig. 4 of Arredouani et al. (2002b).

In summary, the two methods of increasing total Ca^{2+} entry reported in Arredouani et al. (2002b) and simulated here have different effects on the cytosolic Ca^{2+}. These differential effects can be understood with the two-compartment model, and do not require additional features such as CICR.

A compound bursting pattern provides a good test protocol for Ca^{2+} handling

Mixed Ca^{2+} oscillations are sometimes observed in single β-cells or β-cell clusters (Jonkers et al., 1999; Krippeit-Drews et al., 2000) and in islets (Bergsten et al., 1994; Valdeolmillos et al., 1989; Zhang et al., 2003). These oscillations are most likely due to episodes of bursts (Barbosa et al., 1998; Cook 1983; Henquin et al., 1982), which we call compound bursts (Bertram et al., 2004). Compound bursts were mimicked by Arredouani et al. (2002b), and we simulate this protocol in Fig. 7. Here a series of five voltage oscillations is applied, with each oscillation consisting of a 16-s depolarization followed by an 8-s repolarization (Fig. 7 *A*). Two episodes of compound bursts were applied, separated in time by 2 min. In the control conditions, the cytosolic Ca^{2+} nadir rose during the first episode and slowly fell during the time between (Fig. 7 *B*). The slow rise and fall of the nadir reflects the dynamics of the ER Ca^{2+} concentration (Fig. 7 *C*). When the SERCA pumps were disabled ($k_{serca2b} = 0$ and $k_{serca3} = 0$) the ER Ca^{2+} concentration remained flat, and consequently there was no rise in the nadir during the oscillations, and *C* immediately returned to its baseline value at the end of an episode of bursts (Fig. 7 *B*, *dashed line*). These results are consistent with data shown in Fig. 6, *B* and *C*, of Arredouani et al. (2002b).

The impact of the ER on the rise and fall of the Ca^{2+} nadir is further demonstrated in Fig. 8, where the rate of change of C_{er} has been modified by adjusting the fraction of free Ca^{2+} in the ER (f_{er}). First, the speed of the ER was increased by a factor of 10 by changing f_{er} from 0.01 to 0.1 (*solid curves*). In this case, the slow increase in C_{er} exhibited previously during a compound burst (Fig. 7 *C*) is replaced by oscillations in C_{er} around an elevated, but constant, mean. As a result, the cytosolic Ca^{2+} nadir rises quickly during a bursting episode, exhibiting no slow upward ramp (Fig. 8 *A*). Also, with the faster ER the cytosolic Ca^{2+} falls quickly to its baseline value at the end of a compound burst, reflecting the rapid decline in C_{er} (Fig. 8 *B*). To examine the other extreme, we decreased the speed of the ER by a factor of 50, setting $f_{er} = 0.0002$ (*dashed curves*). In this case, the free ER Ca^{2+} concentration increases only slightly during a compound burst, and as a consequence the cytosolic Ca^{2+} nadir returns to baseline between each depolarization, so there is little elevation of the nadir. Thus, a very slow ER has effects on cytosolic Ca^{2+} that are in some ways similar to the effects of disabling the SERCA pumps. One key difference, however, is that the *C* amplitude is larger than that of the control when SERCA pumps are disabled (Fig. 7 *B*), whereas the amplitude is smaller than control when the ER dynamics are slowed by decreasing f_{er} (Fig. 8 *A*). This is because the filtering performed by the ER is reduced in the former case and increased in the latter case.

In summary, the compound bursting simulations in conjunction with the experimental data of Arredouani et al. (2002b) show clearly the influence that the ER has on the cytosolic Ca^{2+} dynamics, both during an episode of bursts and between episodes. They also put constraints on the speed of the ER. If the ER fills and empties too rapidly or too slowly, the slow rise and fall of the Ca^{2+} nadir, which was shown clearly in Arredouani et al. (2002b), is not produced.

Although decreasing the speed of the ER by increasing its filtering capacity greatly reduces the rise in the cytosolic Ca^{2+} nadir during a compound burst, it also decreases the Ca^{2+} amplitude, in contrast to the increase produced when SERCA pumps are inhibited. Indeed, blocking SERCA pumps is the only manipulation we have found that suppresses the rise in the Ca^{2+} nadir while increasing the Ca^{2+} amplitude.

The Ca^{2+} response is inconsistent with experimental data when CICR is a dominant factor

We next investigate the potential role of Ca^{2+}-induced Ca^{2+} release (CICR) in β-cells, by making the rate of efflux from the ER, p_{er}, an increasing function of the cytosolic Ca^{2+} concentration (Eq. 6). The extent of the contribution of CICR to the total release from the ER depends on the choice of parameters. The parameter p_{min} sets the passive release, whereas the magnitude of CICR is determined by $p_{max}-p_{min}$. For example, if $p_{min} = p_{max}$ then CICR will contribute nothing to $J_{release}$. Figures shown thus far have used the basic two-compartment model, where release is passive. All results can be reproduced by a model in which some degree of CICR is included (not shown). However, since CICR tends to reduce the ER Ca^{2+} concentration relative to that in the cytosol, the effects of blocking SERCA pumps are blunted when CICR is included.

We consider now an extreme case, in which $J_{release}$ is dominated by CICR. We saw previously that when release is passive the ER fills during depolarization and drains during repolarization. On the contrary, when release is dominated by CICR the Ca^{2+} entering the cell during depolarization induces release from the ER, so the ER initially fills, but then releases once the cytosolic concentration becomes sufficiently large. During repolarization the ER fills since the cytosolic Ca^{2+} is lower, inducing less release. The response to a train of three depolarizations is demonstrated in Fig. 9.

This CICR model was used to simulate the Ca^{2+} response during the biphasic voltage protocol (Fig. 10 *A*). Except for an initial transient period during which the ER was filling, blocking SERCA pumps had little effect on either the Ca^{2+} nadir or the Ca^{2+} amplitude (Fig. 10 *B*). That is, C returned to baseline after each depolarization, whether SERCA pumps were activated or disabled, and the Ca^{2+} amplitude was slightly decreased when SERCA pumps were blocked. The nadir was not elevated because with this model the ER takes up Ca^{2+} during the repolarized phase, and it is release of Ca^{2+} that produces the elevated nadir. The amplitude was abnormally large because the ER does not take up Ca^{2+} when the cell is depolarized; instead it amplifies the cytosolic Ca^{2+}. Thus, a model in which CICR dominates release from the ER does not reproduce the experimental Tg data (Arredouani et al., 2002b; Gilon et al., 1999).

Continuous depolarization data support the subspace model

The simulations presented thus far highlight dynamic or time-dependent properties of Ca^{2+} handling. A much simpler simulation, continuous depolarization, highlights steady-state properties and yields some surprising results. During continuous depolarization with elevated K^+, Table 1 of Arredouani et al. (2002b) shows that the cytosolic Ca^{2+} concentration was lower in the presence of Tg. Although they did not report this difference as statistically significant, we note that reductions were observed in each of eight conditions. A statistically significant reduction in steady-state Ca^{2+} in the presence of Tg was reported in single β-cells by Lemmens et al. (2001).

Contrary to these data, the basic two-compartment model indicates that the steady-state values should be identical whether or not pumps are blocked. This is easily seen from the equations. At steady state, Eq. 5 yields

$$J_{release} = J_{SERCA} \tag{14}$$

and combined with Eq. 4 we obtain

$$J_{pmca} = J_{ion}; \tag{15}$$

so from Eq. 1,

$$C_\infty = \frac{-\alpha I_{Ca}}{k_{pmca}}, \tag{16}$$

where C_∞ is the equilibrium or steady-state cytosolic Ca^{2+} concentration. Thus, the steady state depends only on the Ca^{2+} influx and efflux across the plasma membrane, and is independent of the ER Ca^{2+} concentration or any parameters relating to the ER. This is true whether release from the ER is passive, as in our basic model, or active through CICR. Thus, the two-compartment models fail to reproduce the continuous depolarization data (Arredouani et al., 2002b; Lemmens et al., 2001).

A three-compartment model has been developed (Goforth et al., 2002) to explain recent data on the buildup and decay of a Ca^{2+}-activated K^+ current during a burst of short action-potential-like depolarizations (Goforth et al., 2002; Göpel et al., 1999; Kanno et al., 2002). As described in Methods, this model contains an ER compartment, a bulk cytosolic compartment, and a Ca^{2+} subspace postulated to exist between the ER and the plasma membrane. In this model, most of the release from the ER enters the subspace compartment, so that the Ca^{2+} concentration in this compartment is elevated above that of the bulk cytosol (Fig. 1 *B*). Like the basic two-compartment model, the three-compartment subspace model reproduces all the experimental data related to the dynamics of Ca^{2+} handling (not shown). However, whereas the two-compartment model (with or without CICR) fails to reproduce the steady-state Ca^{2+} data, the subspace model correctly predicts a decrease in cytosolic Ca^{2+} when SERCA pumps are blocked.

Fig. 11 shows the Ca^{2+} concentrations in the three compartments during a continuous depolarization from −70 to −30 mV. Also shown is C_{avg}, the weighted average of the bulk cytosolic Ca^{2+} (C) and the subspace Ca^{2+} (C_{ss}) concentrations (Eq. 13). This weighted average is what would be observed in experiments measuring the Ca^{2+} concentration in the cell. As with the two-compartment model, the bulk cytosolic Ca^{2+} attains the same steady-state level whether or not the SERCA pumps are inhibited (Fig. 11 *C*), since the steady-state concentration in this compartment satisfies Eq. 16. However, the subspace Ca^{2+} concentration has a lower steady-state value when SERCA pumps are blocked (*dashed line*, Fig. 11 *D*) since the Ca^{2+} influx to this compartment is less when the ER is depleted (Fig. 11 *B*). In fact, the steady-state subspace concentration equals the bulk cytosolic concentration when SERCA pumps are blocked, whereas it is higher when the subspace is intact. Since the observable C_{avg} is the weighted average of C and C_{ss}, it is lower when SERCA pumps are inhibited than in the control case (Fig. 11 *A*), consistent with the experimental data.

DISCUSSION

We have demonstrated that a simple two-compartment model with passive Ca^{2+} release from the ER can reproduce recent time-dependent Ca^{2+} data (Arredouani et al., 2002a,b; Gilon et al., 1999). Although a modest contribution of CICR is compatible with the data, a model in which CICR is the dominant efflux pathway from the ER is not compatible.

Although the two-compartment model, with or without modest CICR, reproduces the time-dependent data, it is not compatible with steady-state Ca^{2+} data showing that the cytosolic Ca^{2+} concentration is lower when SERCA pumps are inhibited by Tg (Arredouani et al., 2002b; Lemmens et al., 2001). Prolonged stimulation with high KCl can produce an atypical form of CICR that does not involve the IP_3R or RyR in normal mouse β-cells (Beauvois et al., 2004). This could lead to a reduction in cytosolic Ca^{2+} when SERCA pumps are blocked. However, we note that the atypical CICR only gives a single, transient release in response to a maintained stimulus (Beauvois et al., 2004), which suggests that CICR is not the best explanation for the steady-state reduction. Here, we have shown a three-compartment model that includes a subspace compartment between the ER and the plasma membrane reproduces both the time-dependent and the steady-state data without recourse to CICR.

This subspace model was developed to account for data showing a transient rise and fall of a current tail that develops during a short train of action-potential-like depolarizations (Goforth et al., 2002), and that has been attributed largely to a voltage-independent, Ca^{2+}-activated K^+ current (Goforth et al., 2002; Göpel et al., 1999; Kanno et al., 2002). The subspace model accounts for this data, whereas the basic two-compartment model does not. If CICR is added to the two-compartment model and is the dominant factor in release, then the $I_{K(slow)}$ data is reproduced. That is, if a substantial part of the rise in cytosolic Ca^{2+} that activates $I_{K(slow)}$ is due to release from the ER, then Tg would reduce $I_{K(slow)}$. However, we have shown here that a model with dominant CICR is not compatible with time-dependent Ca^{2+} data. Thus, in our view, the subspace model most accurately reflects the handling of Ca^{2+} in pancreatic β-cells.

The ER serves as both a Ca^{2+} sink and source. When the cell is depolarized Ca^{2+} enters the cell through ion channels, elevating the cytosolic Ca^{2+} concentration. This causes the ER to take up Ca^{2+}, therefore acting as a sink, which slows and blunts the rise in cytosolic Ca^{2+}. When the cell is repolarized the influx through ion channels stops and the cytosolic Ca^{2+} concentration drops due to removal through membrane Ca^{2+} pumps. As a result Ca^{2+} is released from the ER, which now acts as a source and slows and antagonizes the fall in cytosolic Ca^{2+}. These dual roles provide the framework for understanding the effects of agents known to modify Ca^{2+} pathways in β-cells. For example, when Tg is used to block SERCA pumps, the ER will not have any active uptake mechanism and will no longer serve as a Ca^{2+} sink. Also, since the ER does not fill with Tg present, it will not serve as a Ca^{2+} source when the cell is repolarized. These two effects of SERCA pump blockage can explain all the time-dependent Tg data.

Knockout experiments (Arredouani et al., 2002b) show that ER sourcing and sinking is also eliminated by removal of SERCA3 alone. Thus, this low affinity isoform is solely responsible for ER Ca^{2+} oscillations and their attendant effects on cytosolic Ca^{2+}. The high affinity isoform, SERCA2b, is likely nearly saturated at basal Ca^{2+} and accounts for the ability of the ER to fill, albeit slowly, in low Ca^{2+}, provided sufficient ATP is present (Tengholm et al., 2001).

In addition to accounting for the known data, we have made some new predictions. The model predicts that agents such as carbachol, that increase the release from the ER, will have no long-term effects on the cytosolic Ca^{2+} dynamics. This prediction can readily be tested. Other agents such as Li^+ or calmidazolium reduce efflux across the plasma membrane (Nadal et al., 1994; Wolf et al., 1988) and are predicted to increase the Ca^{2+} nadir, but have no effect on the Ca^{2+} amplitude during the biphasic burst-like voltage protocol.

Finally, we have demonstrated that the cytosolic Ca^{2+} dynamics are affected greatly by the speed at which the ER takes up and releases Ca^{2+}. If the ER is too fast then it will not contribute a slow component to the cytosolic Ca^{2+} dynamics. This slow component is evident in the slow fall of Ca^{2+} often observed after bursts of action potentials in free-running (not voltage-clamped) islets (Gilon et al., 1999; Nadal et al., 1994; Valdeolmillos et al., 1989; Zhang et al., 2003). If the ER is too slow then it will take up only a small amount of Ca^{2+} during burst-like depolarizations. This will have an effect on cytosolic Ca^{2+} that is somewhat similar to the effect of having

no ER compartment at all (i.e., SERCA pumps blocked), and subsequently the ER will not contribute any observable slow component to the Ca^{2+} signal. Thus, the uptake and release of Ca^{2+} from the ER must be slow compared to the timescale of cytosolic Ca^{2+}, but not too slow.

There is experimental evidence that a store-operated current (SOC) is activated in β-cells when the ER is drained either through activation of IP_3 receptors or through inhibition of SERCA pumps (Mears and Zimliki, 2004; Miura et al., 1997; Worley et al., 1994b). This is a non-selective current, permeable to Ca^{2+} as well as other ions (Mears and Zimliki, 2004; Worley et al., 1994a). Although we have not included SOC in the simulations presented here, we have performed simulations to test its effects on the time-dependent Ca^{2+} dynamics (not shown). The extra Ca^{2+} that enters the model cell through SOC when the ER is depleted elevates both the Ca^{2+} peak and the Ca^{2+} nadir when the burst-like depolarization protocol is applied. However, if the Ca^{2+} component of SOC is relatively small, then the overall effect of draining the ER is to reduce the Ca^{2+} nadir. The Ca^{2+} amplitude is increased when the ER is drained regardless of the size of SOC. Also, the Ca^{2+} component of SOC increases the cytosolic Ca^{2+} concentration during long depolarizations when the ER is drained. Thus, the Tg-induced reduction in the Ca^{2+} concentration during long depolarizations reported by Arredouani et al. (2002b) and Lemmens et al. (2001) may be partially blunted by SOC; without SOC the reduction in Ca^{2+} concentration would be even greater. This provides additional support for the three-compartment subspace model, the only model that predicts a reduction in the steady-state cytosolic Ca^{2+} concentration when Tg is present. In this way, the effects of SOC make the case for a three-compartment subspace model more compelling.

This work was partially supported by National Science Foundation grant DMS-0311856 to R. Bertram.

REFERENCES

Ämmälä, C., P.-O. Larsson, P.-O. Berggren, K. Bokvist, L. Juntti-Berggren, H. Kindmark, and P. Rorsman. 1991. Inositol trisphosphate-dependent periodic activation of a Ca^{2+}-activated K^+ conductance in glucose-stimulated pancreatic β-cells. *Nature*. 353:849–852.

Arredouani, A., Y. Guiot, J.-C. Jonas, L. H. Liu, M. Nenquin, J. A. Pertusa, J. Rahier, J.-F. Rolland, G. E. Shull, M. Stevens, F. Wuytack, J. C. Henquin, and P. Gilon. 2002a. SERCA3 ablation does not impair insulin secretion but suggests distinct roles of different sarcoendoplasmic reticulum Ca^{2+} pumps for Ca^{2+} homeostasis in pancreatic β-cells. *Diabetes*. 51:3245–3253.

Arredouani, A., J.-C. Henquin, and P. Gilon. 2002b. Contribution of the endoplasmic reticulum to the glucose-induced $[Ca^{2+}]_c$ response in mouse pancreatic islets. *Am. J. Physiol.* 282:E982–E991.

Ashcroft, F. M., and P. Rorsman. 1989. Electrophysiology of the pancreatic β-cell. *Prog. Biophys. Mol. Biol.* 54:87–143.

Barbosa, R. M., A. M. Silva, A. R. Tomé, J. A. Stamford, R. M. Santos, and L. M. Rosário. 1998. Control of pulsatile 5-HT/insulin secretion from single mouse pancreatic islets by intracellular calcium dynamics. *J. Physiol.* 510:135–143.

Beauvois, M. C., A. Arredouani, J.-C. Jonas, J.-F. Rolland, F. Schuit, J. C. Henquin, and P. Gilon. 2004. Atypical Ca^{2+}-induced Ca^{2+} release from a sarco-endoplasmic reticulum Ca^{2+}-ATPase 3-dependent Ca^{2+} pool in mouse pancreatic β-cells. *J. Physiol.* 559:141–156.

Bergsten, P., E. Grapengiesser, E. Gylfe, A. Tengholm, and B. Hellman. 1994. Synchronous oscillations of cytoplasmic Ca^{2+} and insulin release in glucose-stimulated pancreatic islets. *J. Biol. Chem.* 269:8749–8753.

Bertram, R., L. Satin, M. Zhang, P. Smolen, and A. Sherman. 2004. Calcium and glycolysis mediate multiple bursting modes in pancreatic islets. *Biophys. J.* 87:3074–3087.

Bertram, R., P. Smolen, A. Sherman, D. Mears, I. Atwater, F. Martin, and B. Soria. 1995. A role for calcium release-activated current (CRAC) in cholinergic modulation of electrical activity in pancreatic β-cells. *Biophys. J.* 68:2323–2332.

Cook, D. L. 1983. Isolated islets of Langerhans have slow oscillations of electrical activity. *Metabolism*. 32:681–685.

Gall, D., and I. Susa. 1999. Effect of Na/Ca exchange on plateau fraction and $[Ca]_i$ in models for bursting in pancreatic β-cells. *Biophys. J.* 77:45–53.

Gilon, P., A. Arredouani, P. Gailly, J. Gromada, and J.-C. Henquin. 1999. Uptake and release of Ca^{2+} by the endoplasmic reticulum contribute to the oscillations of the cytosolic Ca^{2+} concentration triggered by Ca^{2+} influx in the electrically excitable pancreatic β-cell. *J. Biol. Chem.* 274: 20197–20205.

Gilon, P., M. Nenquin, and J. C. Henquin. 1995. Muscarinic stimulation exerts both stimulatory and inhibitory effects on the concentration of cytoplasmic Ca^{2+} in the electrically excitable pancreatic β-cell. *Biochem. J.* 311:259–267.

Goforth, P. B., R. Bertram, F. A. Khan, M. Zhang, A. Sherman, and L. S. Satin. 2002. Calcium-activated K^+ channels of mouse β-cells are controlled by both store and cytoplasmic Ca^{2+}: experimental and theoretical studies. *J. Gen. Physiol.* 114:759–769.

Göpel, S. O., T. Kanno, S. Barg, L. Eliasson, J. Galvanovskis, E. Renström, and P. Rorsman. 1999. Activation of Ca^{2+}-dependent K^+ channels contributes to rhythmic firing of action potentials in mouse pancreatic β-cells. *J. Gen. Physiol.* 114:759–769.

Gromada, J., J. Frøkjær-Jensen, and S. Dissing. 1996. Glucose stimulates voltage- and calcium-dependent inositol trisphosphate production and intracellular calcium mobilization in insulin-secreting βTC3 cells. *Biochem. J.* 314:339–345.

Henquin, J. C., H. P. Meissner, and W. Schmeer. 1982. Cyclic variations of glucose-induced electrical activity in pancreatic β-cells. *Pflugers Arch.* 393:322–327.

Jonkers, F. C., J.-C. Jonas, P. Gilon, and J. C. Henquin. 1999. Influence of cell number on the characteristics and synchrony of Ca^{2+} oscillations in clusters of mouse pancreatic islet cells. *J. Physiol.* 520:839–849.

Kang, G., and G. G. Holz. 2003. Amplification of exocytosis by Ca^{2+}-induced Ca^{2+} release in INS-1 pancreatic β-cells. *J. Physiol.* 546:175–189.

Kanno, T., P. Rorsman, and S. O. Göpel. 2002. Glucose-dependent regulation of rhythmic action potential firing in pancreatic β-cells by K_{ATP}-channel modulation. *J. Physiol.* 545:501–507.

Krippeit-Drews, P., M. Dufer, and G. Drews. 2000. Parallel oscillations of intracellular calcium activity and mitochondrial membrane potential in mouse pancreatic β-cells. *Biochem. Biophys. Res. Commun.* 267:179–183.

Lemmens, R., O. Larsson, P.-O. Berggren, and M. S. Islam. 2001. Ca^{2+}-induced Ca^{2+} release from the endoplasmic reticulum amplifies the Ca^{2+} signal mediated by activation of voltage-gated L-type Ca^{2+} channels in pancreatic β-cells. *J. Biol. Chem.* 276:9971–9977.

Mears, D., and C. L. Zimliki. 2004. Muscarinic agonists activate Ca^{2+} store-operated and -independent ionic currents in insulin-secreting HIT-T15 cells and mouse pancreatic β-cells. *J. Membr. Biol.* 197:59–70.

Meissner, H. P., and I. Atwater. 1976. The kinetics of electrical activity of β-cells in response to ''square wave'' stimulation with glucose or glibenclamide. *Horm. Metab. Res.* 8:11–15.

Miura, Y., J. C. Henquin, and P. Gilon. 1997. Emptying of intracellular Ca^{2+} stores stimulates Ca^{2+} entry in mouse pancreatic β-cells by both direct and indirect mechanisms. *J. Physiol.* 503:387–398.

Nadal, A., M. Valdeolmillos, and B. Soria. 1994. Metabolic regulation of intracellular calcium concentration in mouse pancreatic islets of Langerhans. *Am. J. Physiol.* 30:E769–E774.

Tengholm, A., B. Hellman, and E. Gylfe. 2001. The endoplasmic reticulum is a glucose-modulated high-affinity sink for Ca^{2+} in mouse pancreatic β-cells. *J. Physiol.* 530:533–540.

Valdeolmillos, M., R. M. Santos, D. Contreras, B. Soria, and L. M. Rosario. 1989. Glucose-induced oscillations of intracellular Ca^{2+} concentration resembling electrical activity in single mouse islets of Langerhans. *FEBS Lett.* 259:19–23.

Varadi, A., and G. A. Rutter. 2002. Dynamic imaging of endoplasmic reticulum Ca^{2+} concentration in insulin-secreting MIN6 cells using recombinant targeted chameleons: roles of sarco(endo)plasmic reticulum Ca^{2+}-ATPase (SERCA)$^{-2}$ and ryanodine receptors. *Diabetes.* 51:S190–S201.

Wolf, B. A., J. R. Colca, J. Turk, J. Florholmen, and M. L. McDaniel. 1988. Regulation of Ca^{2+} homeostasis by islet endoplasmic reticulum and its role in insulin secretion. *Am. J. Physiol.* 17:E121–E136.

Worley, J. F., M. S. McIntyre, B. Spencer, and I. D. Dukes. 1994a. Depletion of intracellular Ca^{2+} stores activates a maitotoxin-sensitive nonselective cationic current in β-cells. *J. Biol. Chem.* 269:32055–32058.

Worley, J. F., M. S. McIntyre, B. Spencer, R. J. Mertz, M. W. Roe, and I. D. Dukes. 1994b. Endoplasmic reticulum calcium store regulates membrane potential in mouse islet β-cells. *J. Biol. Chem.* 269:14359–14362.

Zhang, M., P. Goforth, A. Sherman, R. Bertram, and L. Satin. 2003. The Ca^{2+} dynamics of isolated mouse β-cells and islets: implications for mathematical models. *Biophys. J.* 84:2852–2870.